

Article

# Enhanced Phenol Tert-Butylation Reaction Activity over Hierarchical Porous Silica-Alumina Materials

Ling Xu <sup>1</sup>, Fan Wang <sup>1</sup>, Zhi Xiu <sup>1</sup>, Limei Duan <sup>1</sup>, Zongrui Liu <sup>1,\*</sup> and Jingqi Guan <sup>2,\*</sup> 

<sup>1</sup> College of Chemistry and Materials Science, Inner Mongolia University for Nationalities, Tongliao 028000, Inner Mongolia, China; tlxuling1979@imun.edu.cn (L.X.); wf18848176887@163.com (F.W.); CH15144964232@163.com (Z.X.); duanlm@imun.edu.cn (L.D.)

<sup>2</sup> Key Laboratory of Surface and Interface Chemistry of Jilin Province, College of Chemistry, Jilin University, Changchun 130012, China

\* Correspondence: liuzr@imun.edu.cn (Z.L.); guanjq@jlu.edu.cn (J.G.); Tel.: +86-0475-8313570 (Z.L.)

Received: 28 July 2020; Accepted: 16 September 2020; Published: 22 September 2020



**Abstract:** Hierarchical aluminum-silicon materials have been successfully prepared by mixing pre-crystallization of silica-alumina sol and citric acid under hydrothermal conditions. The influence of pre-crystallization time on the micro-mesoporous structure is studied using Fourier transform infrared spectroscopy (FT-IR), X-ray powder diffraction (XRD), N<sub>2</sub> physical adsorption, and high-resolution transmission electron microscopy (HRTEM). The catalytic performance of hierarchical silica-alumina material is evaluated by alkylation of phenol with tert-butanol. The results show that the silica-alumina materials with a pre-crystallization time of 16 h show micro-mesoporous structure and excellent catalytic activity.

**Keywords:** hierarchical pore; micro-mesoporous silica-alumina; phenol tert-butylation; pre-crystallization time

## 1. Introduction

As a commonly used material for adsorption separation and catalysis, molecular sieves can be simply divided into three types: micropore, mesopore, and macropore. The pores with a diameter of less than 2 nm, 2–50 nm, and more than 50 nm were called micropores, mesopores, and macropores, respectively [1–3]. With the advancement of research, researchers have gradually discovered that molecular sieves of three pore size have their own characteristics. However, materials with a certain pore structure applied separately in the fields of catalysis, petrochemicals, and ion exchange were usually not ideal [4–8]. For example, the widely used ZSM-5 molecular sieve had a strong acidity and excellent channel selectivity [9–14]. However, the narrow pore size of ZSM-5 limited the transfer and diffusion of macro reactants and products [15–20]. However, the pore walls of the mesoporous materials were amorphous, and the acidity of the materials was relatively low. Therefore, mesoporous materials had poor catalytic activity in acid-catalyzed reactions [21–23].

Due to the shortcomings of single microporous and mesoporous materials in catalytic reactions, many researchers were committed to the composite research of microporous and mesoporous materials [24,25]. Mesoporous template was added into synthetic microporous silica-alumina precursor, which was adopted in situ synthesis method to prepare micro-mesoporous silica-alumina materials. Moreover, the pore wall of the mesoporous silica-alumina material was crystallized, which was named the post-synthesis method [26–28]. In situ synthesis mainly included single template synthesis and double template synthesis [29]. The method was easy to operate, but micropores and mesopores were not well compounded and were easy to separate, leading to the synthesis of a single microporous material or mesoporous material. The post-synthesis method mainly included the pore wall crystallization

method, epitaxial growth method, and alkali treatment method [30]. These methods need be completed in at least two steps, so the preparation methods were more complicated. In our previous work, we used polyethylene glycol as the mesoporous soft template to synthesize hierarchical ZSM-5 zeolites [21]. However, there were two kinds of acid sites, which would result in side reactions. In this work, we used citric acid as the mesoporous template to synthesize hierarchical ZSM-5 zeolites with main single kind of acid site, which favors improvement of the selectivity.

Micro-mesoporous silica-alumina materials obtained by pre-crystallization and an in situ synthesis method can effectively avoid the defects of in situ synthesis and post-synthesis methods. The aluminum-silicon was crystallized at different times to prepare pre-crystallization product with a microporous structural unit or a microporous nanocrystal. The mesoporous pore-forming agent citric acid and the pre-crystallized product were self-assembled under hydrothermal conditions to prepare a micro-mesoporous silica-alumina material.

## 2. Results and Discussion

Figure 1 shows the XRD patterns of the materials. When the pre-crystallization time of the silica-alumina sol is 0 h and 4 h, a broad diffraction peak appeared at  $2\theta = 20\text{--}30^\circ$ , indicating that the silica-alumina sol pre-crystallization time is too short to form a ZSM-5 nano-structure. When the pre-crystallization time is extended to more than 8 h, the sample exhibits characteristic diffraction peaks at  $2\theta = 8.0^\circ, 8.8^\circ, 3.2^\circ, 24.0^\circ$  and  $24.5^\circ$ . It is consistent with the XRD diffraction peaks of ZSM-5 zeolite in the literature [31], which indicates that the prepared materials have the crystal structure of ZSM-5 molecular sieve. With the increase of crystallization time, the intensity of ZSM-5 diffraction peaks gradually increases, suggesting that the crystallization degree of samples increases [32,33].

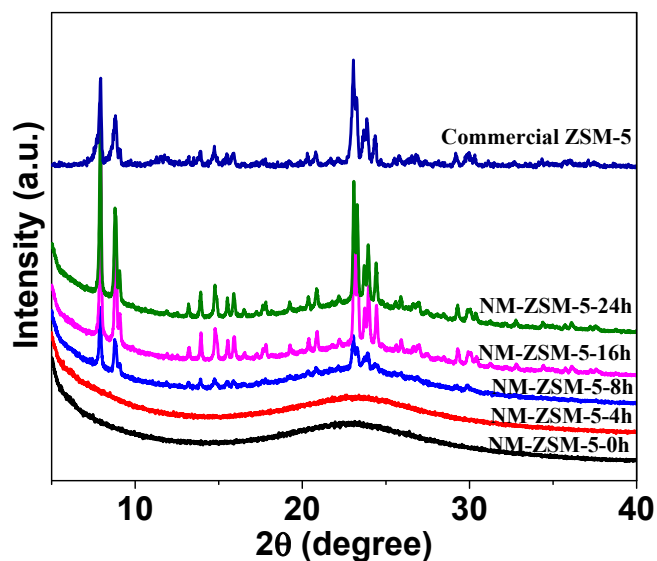
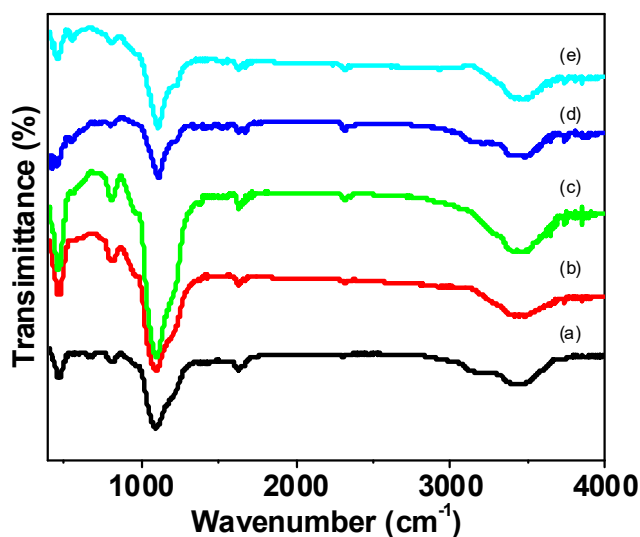


Figure 1. XRD patterns of the samples.

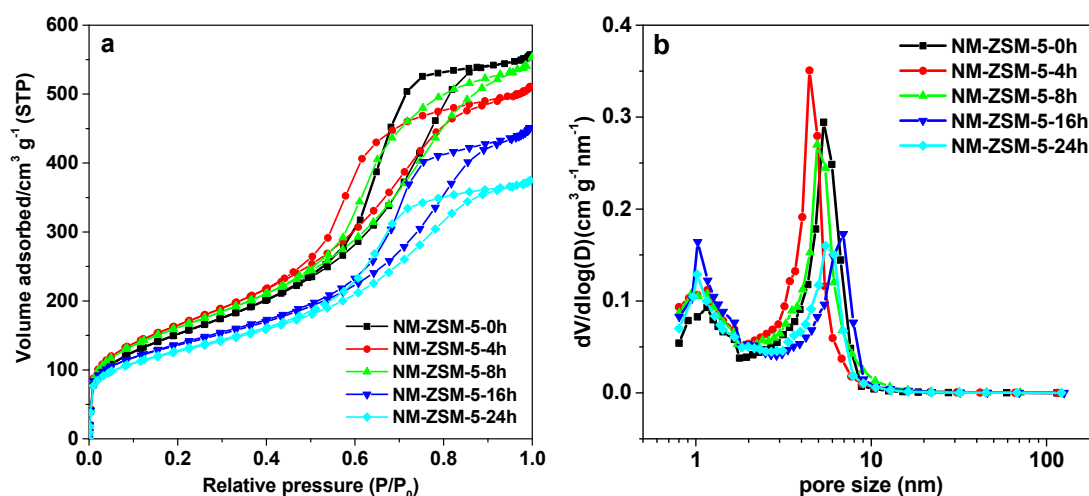
Figure 2 shows the FT-IR spectra of the samples. The absorption peak at  $465\text{ cm}^{-1}$  is ascribed to Si–O–Si (Al) variable angle bending vibration, while the absorption peak at  $810\text{ cm}^{-1}$  belongs to Si–O–Si (Al) symmetric stretching vibration. Moreover, the peak at  $1080\text{ cm}^{-1}$  is due to Si–O–Si (Al) anti-symmetric stretching vibration, whereas the bands at  $1639\text{ cm}^{-1}$  and  $3430\text{ cm}^{-1}$  are attributed to O–H bond bending vibration of water and Si–OH or O–H bond stretching vibration of water, respectively [34]. For pre-crystallization micro-mesoporous materials at 8 h, 16 h, and 24 h, the characteristic peak at  $550\text{ cm}^{-1}$  indicates MFI structure (Figure 2c–e) [34]. However, the ZSM-5 zeolites crystallized at 0 and 4 h do not have this characteristic peak, indicating that the pre-crystallization time is too short and the MFI structure of ZSM-5 is not formed. Therefore, prolonging the pre-crystallization time favors the formation of the microporous structure.



**Figure 2.** FT-IR spectra of (a) NM-ZSM-5-0h, (b) NM-ZSM-5-4h, (c) NM-ZSM-5-8h, (d) NM-ZSM-5-16h, and (e) NM-ZSM-5-24h.

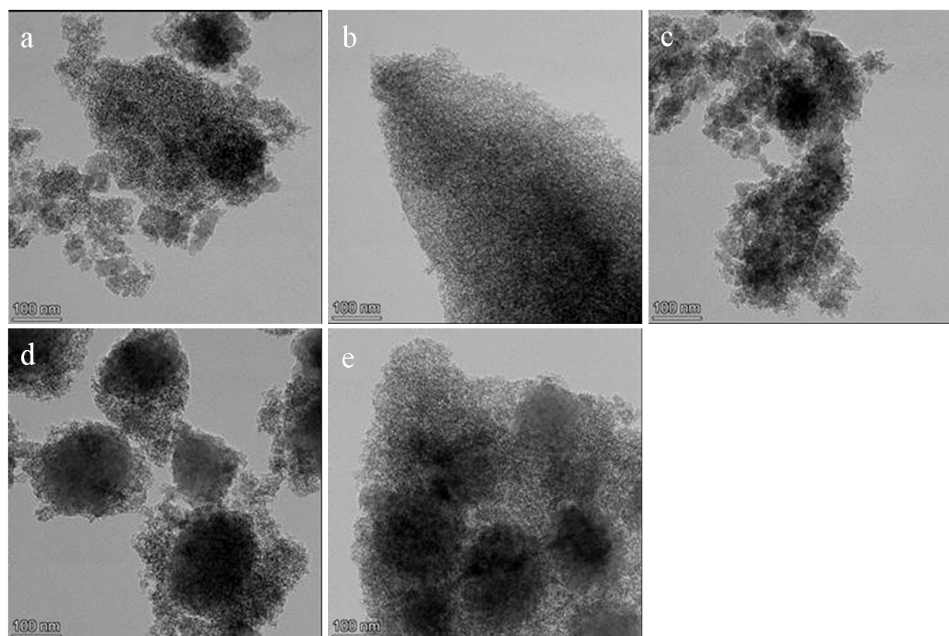
Figure 3 shows the  $N_2$  adsorption-desorption isotherm curves and pore distribution of the samples. It can be seen that the  $N_2$  adsorption-desorption isotherm curves of silica-alumina material is type IV with a  $H_2$  hysteresis ring, indicating that the synthesized samples contain a mesoporous structure. With increasing pre-crystallization time, the hysteresis ring of the isothermal curves becomes smaller, indicating that the crystallinity of the material increases, and the mesoporous order becomes lower. From 0 h to 24 h, the micropore BET specific surface area of the samples gradually decreases from  $547 \text{ m}^2 \text{ g}^{-1}$  to  $440 \text{ m}^2 \text{ g}^{-1}$ . With the increase of pre-crystallization time, the pore specific surface area gradually increases and the mesoporous specific surface area gradually decreases, indicating that the micropore ratio of the samples increases, which is consistent with the results of XRD and FT-IR analysis.

Figure 3b exhibits the pore distribution of the silica-alumina materials. The silica-alumina materials pre-crystallized at different times contain bi-continuous micropore and mesopore distribution. The microporous distribution is mainly centered at about 1 nm, while the mesopore distribution is mainly concentrated at around 6 nm. For the samples with shorter pre-crystallization time (i.e., NM-ZSM-5-0h, NM-ZSM-5-4h and NM-ZSM-5-8h), the distribution of mesopores is relatively concentrated. When the crystallization time is extended to 24 h, the distribution is relatively broad, which is related to the decrease of the mesoporous order degree.



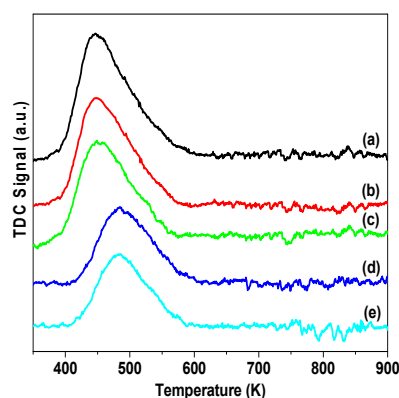
**Figure 3.** (a)  $N_2$  adsorption-desorption isotherms and (b) pore distribution of the samples.

Figure 4 displays TEM images of the samples. The samples with a shorter pre-crystallization time have a uniform structure (Figure 4a–c). With the increase of pre-crystallization time to 24 h, the mesoporous channels gradually change disorder (Figure 4e). The channels are stacked by grains of ZSM-5 nano-crystal.



**Figure 4.** TEM images of (a) NM-ZSM-5-0h, (b) NM-ZSM-5-4h, (c) NM-ZSM-5-8h, (d) NM-ZSM-5-16h, and (e) NM-ZSM-5-24h.

Figure 5 shows the  $\text{NH}_3$ -TPD curves of the samples. All the samples show a  $\text{NH}_3$ -desorption peak. The sample NM-ZSM-5-0h has a broad desorption peak at around 446 K, indicating that the acidity of the sample is weak due to low crystallization [34]. As the pre-crystallization time is prolonged, the desorption peak temperature of  $\text{NH}_3$  gradually increases, indicating that the acidity is enhanced with the increase of microporous crystallinity [35]. For example, for NM-ZSM-5-4h, NM-ZSM-5-8h, NM-ZSM-5-16h, and NM-ZSM-5-24h, the  $\text{NH}_3$ -desorption peak is located at 449 K, 452 K, 485 K, and 486 K, respectively. The desorption peaks of samples NM-ZSM-5-8h, NM-ZSM-5-16h, and NM-ZSM-5-24h can be attributed to the desorption of  $\text{NH}_3$  from medium acid sites [34]. As a whole, the acidity of the hierarchical silicon-alumina material is not strong and suitable for medium-strength acid-catalyzed reactions.



**Figure 5.**  $\text{NH}_3$ -TPD curves of (a) NM-ZSM-5-0h, (b) NM-ZSM-5-4h, (c) NM-ZSM-5-8h, (d) NM-ZSM-5-16h, and (e) NM-ZSM-5-24h.

It was reported that the alkylation of phenol by tert-butanol is an acid-catalyzed reaction. However, the small pore size of microporous molecular sieves such as ZSM-5 (<2 nm) made it very difficult for the large-sized molecule to diffuse effectively in the pore system. Accordingly, the reaction activity of tert-butylation of phenol over the microporous molecular sieves was low. In addition, mesoporous molecular sieve such as Al-MCM-41 has the larger pore channels. However, its catalytic activity is still low, which should be ascribed to weak acidity of amorphous mesoporous walls. It is well known that the micropores in the hierarchical channels system provide acid-catalyzed active centers, while the mesopores and the macropores favor the diffusion of substances and product molecules [36]. The synergistic effect of hierarchical pores could make the complex reaction system efficient, which allows large molecules to coexist with small molecule and is conducive to the formation of the target product. In this work, the alkylation of phenol and tert-butanol is used as a model reaction to investigate the catalytic performance of the hierarchical silica-alumina materials. The phenol tert-butylation reaction is a kind of industrially important acid-catalyzed reaction. The main products, 4-tert-butylphenol (4-TBP) and 2,4-di-tert-butylphenol (2,4-di-TBP), have been widely used in industry as intermediates, such as used in the production of rubber, coatings, antioxidants, thermal stabilizers, and regenerated rubber activators. In addition, the phenol tert-butyl alkylation reaction could be catalyzed by various acids, including Lewis acids and Brønsted acids, such as homogenous liquid acid  $H_3PO_4$ ,  $H_2SO_4$ , HF,  $HClO_4$ , and solid acid catalysts, such as cation exchange resins, zeolites, and mesoporous aluminosilicates. Homogeneous acid catalysts are difficult to recycle, easily corrode equipment, and pollute the environment, and their applications in industry are greatly restricted. Cation exchange resins are easily decomposed and cannot be used at high temperature. Therefore, many researchers invested in microporous zeolites and mesoporous molecular sieves, because they have the advantages of uniform pore size distribution, high thermal stability, and recyclability. The development and application of solid acid catalysts was also of great significance to our environmental protection. In the tert-butylation reaction of phenol, the conversion and selectivity of the product mainly depend on the acidity of the catalyst and the size of the pores. The control of the preparation conditions of the porous silica-alumina material could provide the required pore size and acidity according to the requirements of the reaction. Therefore, it is suitable to use the phenol tert-butylation reaction as a model reaction to investigate the catalytic performance of the hierarchical porous silica-alumina material.

Table 1 shows the catalytic results of the tert-butylation reaction with phenol on the hierarchical silica-alumina materials and compared catalysts. The main products of the reaction are 2-TBP, 4-TBP, 2,4-di-TBP, and a small amount of 2,4,6-tri-TBP. In the alkylation of phenol with tert-butanol, the selectivity depends on the nature of acidic sites in catalysts, reaction temperature and reaction time [37,38]. On weak acidic catalysts, e.g., FIBAN K-1 and KU-2-8 sulfonated cation-exchange resin, oxygen-alkylated product (i.e., phenyl alkyl ether, t-BPE) is formed as a major product [39]. On moderate acidic catalysts, such as ZSM-12 [40], SAPO-11 [41] and zeolite-Y [42], o-isomer (2-TBP), and p-isomer(4-TBP) are mainly formed. In addition, tert-butyl phenyl ether (TBPE) is one of the products in the early stage of the reaction (1–2 h). As the reaction time increases, a decrease in the yield of TBPE and an increase in the yield of TBP (ortho and para isomers) are observed [43]. In our catalytic system, the tert-butyl ether is not obviously observed due to that the product of tert-butylation is withdrawn after reaction for 2 h.

**Table 1.** The compared results of alkylation of phenol with tert-butanol on different catalysts.

Catalysts	$n_{\text{phenol}}/n_{\text{tert-butanol}}$	WHSV ( $\text{h}^{-1}$ )	T ( $^{\circ}\text{C}$ )	Phenol Conversion (%)	Selectivity (%)				Ref.
					2-TBP (%)	4-TBP (%)	2,4-Di-TBP (%)	2,4,6-Tri-TBP (%)	
NM-ZSM-5-0h	0.4	2.20	145	46.1	11.6	70.3	18.0	0.1	This work
NM-ZSM-5-4h	0.4	2.20	145	50.5	12.7	61.3	25.9	0.1	This work
NM-ZSM-5-8h	0.4	2.20	145	65.6	13.5	65.3	21.0	0.2	This work
NM-ZSM-5-16h	0.4	2.20	145	87.5	15.5	62.7	21.6	0.2	This work
NM-ZSM-5-24h	0.4	2.20	145	86.2	15.6	63.2	21.1	0.1	This work
MZ-9-3.2	0.4	2.20	145	96.5	6.2	39.2	53.9	-	[21]
HY	0.5	2.4	200	28.6	11.7	69.7	14.6	-	[37]
HY-550	0.5	2.4	200	62.5	8.5	75.9	9.5	-	[37]
H $\beta$	2	0.67	145	96.2	2.99	76.38	20.63	-	[38]
ZSM-5	0.4	2.2	145	36.7	16.8	42.6	40.6	-	[39]
AIMCM-41(56)	0.5	4.5	175	35.9	8.1	83.4	3.9	-	[40]
H-AIMCM-41	0.5	4.8	215	64.1	1.7	29.9	1.4	-	[40]
FIBAN K1	3	-	100	23	58	33	10	-	[41]

The phenol conversion of NM-ZSM-5-0h and NM-ZSM-5-4h is low due to the weak acidity of pore walls as revealed by the XRD, FT-IR and NH<sub>3</sub>-TPD analysis. The acid was generated by Al<sup>3+</sup> atoms replacing Si<sup>4+</sup> atoms. The lone pair electrons in the Al site generate Lewis acid. To balance the skeleton charge, a hydroxyl is formed on the Al site, which generates the Brønsted acid site. With the pre-crystallization time increasing to 16 h, the catalytic activity of NM-ZSM-5-16h increases. The conversion of phenol increases to 89.5%, which is attributed to that the microporous nanocrystals in the silica-alumina catalyst provide sufficient acid centers for the reaction, suggesting that the phenol tert-butylation reaction can be efficiently catalyzed by medium-strength acid. In addition, the mesoporous structure promotes transfer and diffusion of reactants and products. When the pre-crystallization time reaches 24 h, the catalytic activity of the NM-ZSM-5-24h decreases slightly to 86.2%. From the results of XRD and TEM analysis, it is found that the mesoporous uniformity of the sample NM-ZSM-5-24h decreases, which results in the decrease of catalytic activity. Therefore, the phenol tert-butylation reaction is affected by acid strength and pore structure. Medium-strength acid and suitable mesopores favor this reaction.

The catalytic activity on micropore zeolite (HY [44], H $\beta$  [45], ZSM-5 [46]), mesopore molecular sieve (AIMCM-41) [47], and hierarchical zeolite (MZ-9-3.2) [21] are compared in Table 1. The difference in the activity could be mainly attributed to their different pore structure property and acidity. Hence, proper pore structure and acidity in the hierarchical ZSM-5 zeolite enable easy diffusion of reactants and products, favoring high phenol conversion and high selectivity. It is worth mentioning that the selectivity of the macromolecular 2,4-di-TBP in the products of the hierarchical porous silica-alumina catalyst is low, while the selectivity of the 4-TBP is high, which is consistent with the results of the overall acidity of hierarchical porous silicon-aluminum materials, indicating that the acid center of the medium acidity of the catalyst is more suitable for the formation of 4-TBP. In addition, the formation of 4-TBP might be due to transalkylation from 2-TBP as reported previously [48].

### 3. Experimental Section

#### 3.1. Experimental Reagents

The following reagents were used in this study: Aluminum sulfate octadecahydrate (99.9%, Xilong Chemical Plant, Shantou, Guangdong, China); citric acid (>99.8%, Sinopharm Chemical Reagent Co., Ltd, Shanghai, China); tetrapropylammonium hydroxide (TPAOH) (25%, Wengjiang Chemical Reagent Co., Ltd, Shaogua, Guangdong, China) ethyl orthosilicate (TEOS) (analytical grade, Damao Chemical Reagent Factory, Tianjin, China); ammonium nitrate (analytical grade, Xilong Chemical Plant, Shantou, Guangdong, China); phenol (analytical grade, Damao Chemical Reagent Factory, Tianjin, China); tert-butyl alcohol Sinopharm Chemical Reagent Co., Ltd, Shanghai, China. All the reagents were used as received without further purification.

#### 3.2. Preparation of Materials

##### 3.2.1. Preparation of Microporous-Mesoporous ZSM-5

After 0.1420 g Al<sub>2</sub>(SO<sub>4</sub>)<sub>3</sub>·18H<sub>2</sub>O solid was completely dissolved in 3.75 mL H<sub>2</sub>O, 6.25 mL of tetrapropylammonium hydroxide (TPAOH) was added to the solution. Then it was stirred for 3 h until it became a colorless transparent liquid. 5 mL of tetraethyl orthosilicate (TEOS) was added to the colorless transparent liquid, which was stirred for 9 h to form silica-alumina sol. The sol was transferred into polytetrafluoroethylene-lined reactor and pre-crystallized for different times (0 h, 4 h, 8 h, 16 h and 24 h) in 373 K. Finally, 5.7 g of citric acid was added into the pre-crystallization sol, stirred for 3 h, and crystallized at 373 K for 48 h. After sufficient grinding, the remaining solids were roasted in a muffle furnace at 823 K. According to the pre-crystallization time, the samples were named as NM-ZSM-5-0h, NM-ZSM-5-4h, NM-ZSM-5-8h, NM-ZSM-5-16h, and NM-ZSM-5-24h.

### 3.2.2. Preparation of H-Type Microporous-Mesoporous ZSM-5

The alkylation reaction of phenol and tert-butanol was used as a model reaction, which is a well-known acid-catalyzed reaction using a solid acid as a catalyst. Therefore, the prepared hierarchical porous silicon aluminum materials were treated into acidic H-type solid acid catalysts as follows: 1.5 g of white solid powder after calcination was put into a three-necked flask, and 24 g of ammonium nitrate and 100 mL of distilled water were added. After stirring for 4 h in a 353 K, filtering, and drying at 373 K for 1 h, 1.5 g of the dried product and 24 g of ammonium nitrate was stirred in 100 mL of distilled water at 353 K for 4 h. After filtering and washing, the obtained filter cake was dried at 373 K and then calcined in a muffle furnace at 773 K for 5 h to obtain an H-type microporous-mesoporous silica-alumina catalyst.

### 3.3. Catalyst Characterization

The Fourier Infrared Spectroscopy (FT-IR) was performed on an IRAffinity-IS Fourier Infrared Spectrometer (Shimadzu Corporation, Kyoto, Japan). X-ray powder diffraction (XRD) was performed on a D8 type X-ray powder diffractometer (Bruker, Karlsruhe, Germany). For N<sub>2</sub> physical adsorption, the specific surface area and pore volume of the sample are measured on a Micromeritics ASAP 2010 type adsorber (Micromeritics, Atlanta, GA, USA). The sample was degassed at 573 K for 3 h before the sample was measured. Adsorption is performed at the temperature of liquid nitrogen, and N<sub>2</sub> is the adsorbate. Under relative pressure  $P/P_0 = 0.05\text{--}0.20$ , the BET specific surface area is calculated using the BET equation. The high-resolution transmission electron microscope (TEM) was performed on a Tecnai G2 F20 high-resolution transmission electron microscope (FEI Company, Hillsboro, OR, USA).

### 3.4. Catalytic Tests

The phenol tert-butylation reaction was performed in a fixed-bed a micro-quantitative reactor. 0.5 g of hydrogen-type microporous-mesoporous silica-alumina material was used as the catalyst for the phenol tert-butylation reaction. The reactants of n (phenol): n (tert-butanol) = 1:2.5, the injection speed was 2.2 mL/h, and the reaction temperature was 418 K. The reaction product was dissolved in absolute ethanol, which was analyzed with a gas chromatograph. Using area normalization method, the phenol conversion rate and product selectivity can be obtained.

## 4. Conclusions

In conclusion, we have successfully synthesized hierarchical aluminum-silicon materials by the hydrothermal method and using citric acid as the mesoporous template. The microporous distribution is centered at ca. 1 nm, whereas the mesopore distribution is located at ca. 6 nm. A main single kind of acid site is formed in the as-prepared catalysts. Medium-strength acidity and micro-mesoporous structure are generated in the hierarchical aluminum-silicon materials with a pre-crystallization time of 16 h, which can efficiently catalyze alkylation of phenol with tert-butanol, on which 87.5% of phenol conversion and 62.7% selectivity to 4-di-TBP can be achieved.

**Author Contributions:** Writing—review the manuscript, L.X.; Data collection, F.W.; Data collection, Z.X.; Data interpretation, L.D.; Study design, Z.L.; Writing—review and editing, J.G. All authors have read and agreed to the published version of the manuscript.

**Funding:** This work was financially supported by the National Natural Science Foundation of China (grant no. 21561024 and 21661026).

**Conflicts of Interest:** The authors declare no conflict of interest.

## References

1. Zdravkov, B.D.; Cermak, J.J.; Sefara, M.; Janku, J. Pore classification in the characterization of porous materials: A perspective. *Cent. Eur. J. Chem.* **2007**, *5*, 385–395.

2. Tang, W.; Wang, C.; Yang, X.; Zhang, J. Enhanced phenol degradation using an immobilized highly efficient degrading fungus on a new porous adsorption material. *Energy Sources Part A* **2018**, *40*, 2599–2611. [[CrossRef](#)]
3. Nahakpam, L.; Chipem, F.A.S.; Chingakham, B.S.; Laitonjam, W.S. Diacetoxyiodobenzene assisted C-O bond formation via sequential acylation and deacylation process: Synthesis of benzoxazole amides and their mechanistic study by DFT. *Org. Biomol. Chem.* **2016**, *14*, 7735–7745. [[CrossRef](#)]
4. Zhang, Y.; Zhu, K.; Duan, X.; Li, P.; Zhou, X.; Yuan, W. Synthesis of hierarchical ZSM-5 zeolite using CTAB interacting with carboxyl-ended organosilane as a mesotemplate. *RSC Adv.* **2014**, *4*, 14471–14474. [[CrossRef](#)]
5. Silaghi, M.-C.; Chizallet, C.; Raybaud, P. Challenges on molecular aspects of dealumination and desilication of zeolites. *Microporous Microporous Mater.* **2014**, *191*, 82–96. [[CrossRef](#)]
6. Cremoux, T.; Batonneau-Gener, I.; Moissette, A.; Paillaud, J.L.; Hureau, M.; Ligner, E.; Morais, C.; Laforge, S.; Marichal, C.; Nouali, H. Influence of hierarchization on electron transfers in structured MFI-type zeolites. *Phys. Chem. Chem. Phys.* **2018**, *20*, 26903–26917. [[CrossRef](#)] [[PubMed](#)]
7. Liang, J.; Liang, Z.; Zou, R.; Zhao, Y. Heterogeneous catalysis in zeolites, mesoporous silica, and metal-organic frameworks. *Adv. Mater.* **2017**, *29*, 1701139. [[CrossRef](#)] [[PubMed](#)]
8. Singh, B.; Na, J.; Konarova, M.; Wakihara, T.; Yamauchi, Y.; Salomon, C.; Gawande, M.B. Functional Mesoporous Silica Nanoparticles for Catalysis and Environmental Applications. *Bull. Chem. Soc. Jpn.* **2020**. [[CrossRef](#)]
9. Zhang, X.; Lei, H.; Zhu, L.; Wei, Y.; Liu, Y.; Yadavalli, G.; Yan, D.; Wu, J.; Chen, S. Production of renewable jet fuel range alkanes and aromatics via integrated catalytic processes of intact biomass. *Fuel* **2015**, *160*, 375–385. [[CrossRef](#)]
10. Biriaei, R.; Nohair, B.; Kaliaguine, S. A facile route to synthesize mesoporous ZSM-5 with hexagonal arrays using P123 triblock copolymer. *Microporous Microporous Mater.* **2020**, *298*, 110067. [[CrossRef](#)]
11. Heracleous, E.; Pachatouridou, E.; Hernandez-Gimenez, A.M.; Hernando, H.; Fakin, T.; Paioni, A.L.; Baldus, M.; Serrano, D.P.; Bruijninx, P.C.A.; Weckhuysen, B.M.; et al. Characterization of deactivated and regenerated zeolite ZSM-5-based catalyst extrudates used in catalytic pyrolysis of biomass. *J. Catal.* **2019**, *380*, 108–122. [[CrossRef](#)]
12. Al-Dughaiter, A.S.; Lasa, H.D. HZSM-5 Zeolites with Different SiO<sub>2</sub>/Al<sub>2</sub>O<sub>3</sub> Ratios. Characterization and NH<sub>3</sub> Desorption Kinetics. *Ind. Eng. Chem. Res.* **2014**, *53*, 15303–15316. [[CrossRef](#)]
13. Shen, Y.; Li, H.; Zhang, X.; Wang, X.; Lv, G. The diquatery ammonium surfactant-directed synthesis of single-unit-cell nanowires of ZSM-5 zeolite. *Nanoscale* **2020**, *12*, 5824–5828. [[CrossRef](#)] [[PubMed](#)]
14. Qiao, K.; Zhou, F.; Han, Z.; Fu, J.; Ma, H.; Wu, G. Synthesis and physicochemical characterization of hierarchical ZSM-5: Effect of organosilanes on the catalyst properties and performance in the catalytic fast pyrolysis of biomass. *Microporous Microporous Mater.* **2019**, *274*, 190–197. [[CrossRef](#)]
15. Lee, H.; Zones, S.I.; Davis, M.E. A combustion-free methodology for synthesizing zeolites and zeolite-like materials. *Nature* **2003**, *425*, 385–388. [[CrossRef](#)]
16. Corma, A.; Diaz-Cabanas, M.; Martinez-Triguero, J.; Rey, F.; Rius, J. A large-cavity zeolite with wide pore windows and potential as an oil refining catalyst. *Nature* **2002**, *418*, 514–517. [[CrossRef](#)]
17. Corma, A. From Microporous to Mesoporous Molecular Sieve Materials and Their Use in Catalysis. *Chem. Rev.* **1997**, *97*, 2373–2420. [[CrossRef](#)]
18. Jorge, E.Y.; Lima, C.G.; Lima, T.M.; Marchini, L.; Gawande, M.B.; Tomanec, O.; Varma, R.S.; Paixão, M.W. Sulfonated dendritic mesoporous silica nanospheres: A metal-free lewis acid catalyst for the upgrading of carbohydrates. *Green Chem.* **2020**, *22*, 1754–1762. [[CrossRef](#)]
19. Chiang, W.-S.; Fratini, E.; Baglioni, P.; Georgi, D.; Chen, J.-H.; Liu, Y. Methane Adsorption in Model Mesoporous Material, SBA-15, Studied by Small-Angle Neutron Scattering. *J. Phys. Chem. C* **2016**, *120*, 4354–4363. [[CrossRef](#)]
20. Che, Q.; Yang, M.; Wang, X.; Yang, Q.; Chen, Y.; Chen, X.; Chen, W.; Hu, J.; Zeng, K.; Yang, H.; et al. Preparation of mesoporous ZSM-5 catalysts using green templates and their performance in biomass catalytic pyrolysis. *Bioresour. Technol.* **2019**, *289*, 121729–121737. [[CrossRef](#)]
21. Xu, L.; Wang, F.; Feng, Z.; Liu, Z.; Guan, J. Hierarchical ZSM-5 Zeolite with Enhanced Catalytic Activity for Alkylation of Phenol with Tert-Butanol. *Catalysts* **2019**, *9*, 202. [[CrossRef](#)]
22. Xu, L.; Zhang, Q.; Zhang, M.; Mao, L.; Hu, J.; Liu, Z.; Xie, Y. Synthesis of micro-mesoporous molecular sieve ZSM-5/SBA-15: Tuning aluminium content for tert-butylation of phenol. *J. Chem. Sci.* **2019**, *131*, 42. [[CrossRef](#)]

23. Song, Y.; Hua, Z.; Zhu, Y.; Zhou, J.; Zhou, X.; Liu, Z.; Shi, J. Solvent-free liquid phase tert-butylation of phenol over hierarchical ZSM-5 zeolites for the efficient production of 2,4-ditert-butylphenol. *J. Mater. Chem.* **2012**, *22*, 3327–3329. [[CrossRef](#)]
24. Yang, X.-Y.; Chen, L.-H.; Li, Y.; Rooke, J.C.; Sanchez, C.; Su, B.-L. Hierarchically porous materials: Synthesis strategies and structure design. *Chem. Soc. Rev.* **2017**, *46*, 481–558. [[CrossRef](#)] [[PubMed](#)]
25. White, R.J.; Fischer, A.; Goebel, C.; Thomas, A. A Sustainable Template for Mesoporous Zeolite Synthesis. *J. Am. Chem. Soc.* **2014**, *136*, 2715–2718. [[CrossRef](#)] [[PubMed](#)]
26. Liu, S.; Ren, J.; Zhu, S.; Zhang, H.; Lv, E.; Xu, J.; Li, Y.-W. Synthesis and characterization of the Fe-substituted ZSM-22 zeolite catalyst with high n-dodecane isomerization performance. *J. Catal.* **2015**, *330*, 485–496. [[CrossRef](#)]
27. Liu, S.; Ren, J.; Zhang, H.; Lv, E.; Yang, Y.; Li, Y.-W. Synthesis, characterization and isomerization performance of micro/mesoporous materials based on H-ZSM-22 zeolite. *J. Catal.* **2016**, *335*, 11–23. [[CrossRef](#)]
28. Chen, L.; Xue, T.; Wu, H.; Wu, P. Hierarchical ZSM-5 nanocrystal aggregates: Seed-induced green synthesis and its application in alkylation of phenol with tert-butanol. *RSC Adv.* **2018**, *8*, 2751–2758. [[CrossRef](#)]
29. Shi, C.; Fu, Y.; Chen, W.; Shi, H.; Cong, Y.; Xv, L.; Zhang, D. Microwave hydrothermal synthesis and catalytic cracking of polyethylene of microporous-mesoporous molecular sieves (HY/SBA-15). *Mater. Lett.* **2020**, *258*, 126805. [[CrossRef](#)]
30. Witman, M.; Ling, S.; Boyd, P.; Barthel, S.; Haranczyk, M.; Slater, B.; Smit, B. Cutting Materials in Half: A Graph Theory Approach for Generating Crystal Surfaces and Its Prediction of 2D Zeolites. *ACS Cent. Sci.* **2018**, *4*, 235–245. [[CrossRef](#)]
31. Kim, J.; Choi, M.; Ryoo, R. Effect of mesoporosity against the deactivation of MFI zeolite catalyst during the methanol-to-hydrocarbon conversion process. *J. Catal.* **2010**, *269*, 219–228. [[CrossRef](#)]
32. Khodakov, A.Y.; Zholobenko, V.L.; Imperor-Clerc, M.; Durand, D. Characterization of the initial stages of SBA-15 synthesis by in situ time-resolved small-angle X-ray scattering. *J. Phys. Chem. B* **2005**, *109*, 22780–22790. [[CrossRef](#)] [[PubMed](#)]
33. Freitez, A.; Pabst, K.; Kraushaar-czarnetzki, B.; Schaub, G. Single-Stage Fischer-Tropsch Synthesis and Hydroprocessing: The Hydroprocessing Performance of Ni/ZSM-5/gamma-Al<sub>2</sub>O<sub>3</sub> under Fischer-Tropsch Conditions. *Ind. Eng. Chem. Res.* **2011**, *50*, 13732–13741. [[CrossRef](#)]
34. Xu, L.; Ma, Y.; Ding, W.; Guan, J.; Wu, S.; Kan, Q. Effect of crystallization time on the physico-chemical and catalytic properties of the hierarchical porous materials. *Mater. Res. Bull.* **2010**, *45*, 1293–1298. [[CrossRef](#)]
35. Rodriguez-Gonzalez, L.; Hermes, F.; Bertmer, M.; Rodriguez-Castellon, E.; Jimenez-Lopez, A.; Simon, U. The acid properties of H-ZSM-5 as studied by NH<sub>3</sub>-TPD and Al-27-MAS-NMR spectroscopy. *Appl. Catal. A* **2007**, *328*, 174–182. [[CrossRef](#)]
36. Blin, J.L.; Imperor-Clerc, M. Mechanism of self-assembly in the synthesis of silica mesoporous materials: In situ studies by X-ray and neutron scattering. *Chem. Soc. Rev.* **2013**, *42*, 4071–4082. [[CrossRef](#)]
37. Jiang, T.; Lu, L.; Le, S.; Ma, Y.; Dai, L.; Zhao, H.; Zhao, Q. Improvement of the catalytic activity of MCM-48 synthesized from metakaolinite in the alkylation of phenol with tert-butyl alcohol. *J. Appl. Clay Sci.* **2015**, *109–110*, 1–7. [[CrossRef](#)]
38. Jiang, T.; Cheng, J.; Liu, W.; Fu, L.; Zhou, X.; Zhao, Q.; Yin, H. Sulfuric acid functional zirconium (or aluminum) incorporated mesoporous MCM-48 solid acid catalysts for alkylation of phenol with tert-butyl alcohol. *J. Solid State Chem.* **2014**, *218*, 71–80. [[CrossRef](#)]
39. Anand, R.; Maheswari, R.; Gore, K.U.; Tope, B.B. Tertiary butylation of phenol over HY and dealuminated HY zeolites. *J. Mol. Catal. A Chem.* **2003**, *193*, 251–257. [[CrossRef](#)]
40. Huang, J.H.; Xing, L.H.; Wang, H.S.; Li, G.; Wu, S.J.; Wu, T.H.; Kan, Q.B. Tertiary butylation of phenol over hexagonal p6mm mesoporous aluminosilicates with enhanced acidity. *J. Mol. Catal. A Chem.* **2006**, *259*, 84–90. [[CrossRef](#)]
41. Zhang, K.; Zhang, H.B.; Xu, G.H.; Xiang, S.H.; Xu, D.; Liu, S.Y.; Li, H.X. Alkylation of phenol with tert-butyl alcohol catalyzed by large pore zeolites. *Appl. Catal. A Gen.* **2001**, *207*, 183–190. [[CrossRef](#)]
42. Sakthivel, A.; Badamali, S.K.; Selvam, P. Para-Selective t-butylation of phenol over mesoporous H-ALMCM-41. *Microporous Mesoporous Mater.* **2000**, *39*, 457–463. [[CrossRef](#)]
43. Terekhov, A.V.; Zhanavskina, L.N.; Khadzhiev, S.N. Selecting an optimum catalyst for producing para-tert-butylphenol by phenol alkylation with tert-butanol. *Pet. Chem.* **2017**, *57*, 714–717. [[CrossRef](#)]

44. Chang, C.D.; Hellring, S.D. Para-Selective Butylation of Phenol over Fairly Large-Pore Zeolites. U.S. Patent 5,288,927, 22 February 1994.
45. Subramanian, S.; Mitra, A.; Satyanarayana, C.V.V.; Chakrabarty, D.K. Para-selective butylation of phenol over silicoaluminophosphate molecular sieve sapo-11 catalyst. *Appl. Catal. A Gen.* **1997**, *159*, 229–240. [[CrossRef](#)]
46. Namba, S.; Yashima, T.; Itaba, Y.; Hara, N. Selective formation of p-cresol by alkylation of phenol with methanol over y type zeolite. *Stud. Surf. Sci. Catal.* **1980**, *5*, 105–111.
47. Li, J.; Lou, L.L.; Yang, Y.; Hao, H.; Liu, S. Alkylation of phenol with tert-butyl alcohol over dealuminated HMCM-68 zeolites. *Microporous Mesoporous Mater.* **2015**, *207*, 27–32. [[CrossRef](#)]
48. Chang, J.; Pan, X.; Liu, X.; Xue, Q.; Fu, J.; Zhang, A. The formation of PBDFs from the ortho-disubstituted phenol precursors: A comprehensive theoretical study on the PBDD/Fs formation from 2,4,6-tribromophenol. *Sci. Total Environ.* **2020**, *713*, 136657. [[CrossRef](#)]



© 2020 by the authors. Licensee MDPI, Basel, Switzerland. This article is an open access article distributed under the terms and conditions of the Creative Commons Attribution (CC BY) license (<http://creativecommons.org/licenses/by/4.0/>).